euspen's 25th International Conference & Exhibition, Zaragoza, ES, June 2025
www.euspen.eu

High-precision force sensor for directly SI-traceable and orientation-independent measurements

Martin Wittke[1], Mario André Torres Melgarejo[1], Matthias Wolf[1], Thomas Fröhlich[2], René Theska[1]

Technische Universität Ilmenau, Department of Mechanical Engineering,
[1]Institute for Design and Precision Engineering, Precision Engineering Group
[2]Insitute of Process Measurement and Sensor Technology, Process Metrology Group

E-Mail: martin.wittke@tu-ilmenau.de

Abstract
In 2019, the unit Kilogram of the International System of Units (SI) was redefined by setting Planck's constant to a fixed value of $h = 6.626\,070\,15 \cdot 10^{-34}$ J s. Force and mass measurements have no longer to be traced back by physical references to the International Prototype of the Kilogram. The Kibble Principle enables absolute measurements and provides traceability to Plack's constant, the speed of light, and the caesium standard. The implementation requires systems that correlate electrical and mechanical quantities.
This work features a force sensor for high-precision orientation-independent measurements according to the Kibble Principle. The sensor has been developed for potential applications in high-precision force metrology and micro- and nanofabrication. The structure of the system is based on the Planck Balance, whereby a voice coil actuator and a fiber interferometric sensor ensure SI-traceability. The kinematic structure is designed as a compliant mechanism. To increase the measurement resolution and reduce the measurement uncertainty, sub-mechanisms for compensating the inherent stiffness are integrated. The mechanisms use preloaded springs to ensure functionality in any orientation in the field of gravity. By integrating two almost identical submechanisms, the stiffness and the measurement window can be adjusted consecutively by the preload of the springs. A force measurement resolution of 880 pN is achieved with the current configuration.

Keywords: force sensor, load cell, force compensation, Velocity Mode, stiffness compensation, Kibble Principle, SI-traceability

1. Introduction

Prior to 2019, the traceability of the SI unit kilogram had to be ensured via a long calibration chain back to the International Prototype of the Kilogram. All mass or force measurements therefore referred to one single artifact. By setting Planck's constant to a fixed numerical value of $h = 6.626\,070\,15 \cdot 10^{-34}$ J s as the new SI reference, absolute measurements are enabled. Systems that correlate electrical and mechanical quantities directly with each other are required. There are various approaches, which are mainly used in high-precision mass determination. Well-known examples are the Kibble Balance [1], the Planck Balance [2,6], and the Joule Balance [3]. Further applications can be found for the calibration of cantilevers [4] and ultrasonic power measurements [5].
This work features a newly developed force sensor according to the Kibble Principle. It is intended for applications in high-precision force metrology and micro- and nanofabrication. Starting from the basic structure of a Planck Balance, spring-based submechanisms are implemented to compensate for the stiffness of the compliant kinematic structure. Absolute high-resolution force measurements traceable to the SI are guaranteed independently of the orientation in the gravity field.

2. Approaches

The most advanced force metrology systems can be found in mass metrology. Approaches such as the Kibble Principle including the electromagnetic force compensation and an in-situ actuator calibration as well as stiffness compensation provide the basis for high-precision SI-traceable force measurements.

2.1. Electromagnetic force compensation

To measure absolute force values with reference to the new definition of the SI unit kilogram, electromagnetic force compensation can be used. It requires a kinematic structure and a control loop consisting of a position sensor, a controller, and a voice coil actuator. An artifact with the mass m_A to be measured is initially positioned on the kinematic structure. The resulting deflection is detected by the position sensor, processed by the controller, and converted into a coil current $i_c(t)$. The kinematic structure is moved back to its initial position. According to equation (1), the weight force $F_{G,A}$ of the artifact is compensated by the electrical force $F_{E,Ac}$ of the actuator. The correlation between mechanical and electrical quantities is provided by the actuator constant $B_{VC} \cdot L_{VC}$.

$$F_{G,A} = m_A \cdot g = i_c(t) \cdot B_{VC} \cdot L_{VC} = F_{E,Ac} \quad (1)$$

2.2 Velocity Mode

The Velocity Mode is utilized for the SI-traceable calibration of the Measurement Mode actuator. To determine the actuator constant $B_{VC} \cdot L_{VC}$, an interferometer and a calibration actuator must be integrated into the system. Defined motions are initiated into the system by energizing the calibration actuator with the current $i_{VM}(t)$. The speed $\dot{d}_{PC}(t)$ at a translatory moving link of the kinematic structure and the simultaneously induced voltage $u_{VM}(t)$ in the measurement actuator are measured and synchronized. The actuator constant of the measurement actuator can thus be calculated according to equation (2).

$$u_{VM}(t) = \dot{d}_{PC}(t) \cdot B_{VC} \cdot L_{VC} \quad (2)$$

2.3. Stiffness compensation

To implement highly precise and reproducible motions, kinematic structures in precision engineering applications are usually designed as compliant mechanisms. However, they have the disadvantage of a restoring effect when deflected. For force metrology applications, this stiffness is a highly limiting factor. By reducing the thickness of the thin flexure hinges to a technical minimum of 50 µm [7], the initial stiffness can be minimized. However, further stiffness compensation is required.Masses, magnets and springs are predominantly used to generate the compensation load.. Spring-based systems have the advantage that they function independently of the orientation in the gravity field and do not cause undesired electromagnetic effects. Generally, there are two embodiments. The spring can be preloaded prior to the motion. Due to the load and changing geometric conditions during the motion, the compensation effect is generated. The other option is to not preload the spring initially. The compensation load is created by the motion. For the target application, preloading the spring before the motion is advantageous. It allows the load to be adjusted to the properties of the individual manufactured system.

3. Force sensor structure

The developed force sensor features the concept of the Planck Balance [2,6]. Planck balances are based on the Kibble principle, but target relative uncertainties of around 10^{-8} (k = 1) due to their field of application [6]. Submechanisms are integrated to maximize the sensitivity by compensating for the stiffness of the compliant kinematic structure. The compensation force is generated by a spring. The sensor is realized in a very compact design to enable a wide range of applications. The configuration targets a maximum force resolution with an uncertainty of less than 10^{-5} over a maximum measurement range.

3.1. Concept

The concept of the developed force sensor (Figure 1) features all the main elements of the Planck Balance. This includes the kinematic structure ② consisting of a parallel spring guide, a measurement lever, and a coupling element, the control loop with the position sensor ③, the controller ④, and the voice coil actuator ⑤ as well as the interferometer ⑥ required for the SI-traceable actuator calibration in Velocity Mode. For the intended measurement uncertainty the use of just one actuator to generate the calibration motion and at the same time to evaluate the induced voltage is sufficient [8]. However, the transmission ratio of the measurement lever needs to be characterized precisely since it is a main uncertainty contributor. The force to be measured is applied to a spherical probe ①.

Two almost identical submechanisms ⑦ using preloaded springs are integrated for the compensation of the stiffness of the compliant kinematic structure [9]. The joints P_1 and P_2 are specifically arranged by $\Delta\overline{P_1N_1}$ and $\Delta\overline{P_2N_2}$ outside the connecting line NOQ. On one hand, the stiffness can thus be compensated by equal absolute preload distances $d_{Qx,n}$ with a higher resolution compared to a single submechanism. Additionally, the function-limiting shift of the measurement window resulting from manufacturing deviations [10] can be adjusted. Therefore, the set preload distances $d_{Qx,n}$ are adjusted relative to each other by the same amount in contrary directions. The moments around the joints P_1 and P_2 M_{P1} and M_{P2} (Equations (3) and (4)) are set to equal magnitude and opposite rotation directions. The set stiffness remains at the initially adjusted value.

$$M_{P1} = C_S \cdot d_{Qx,1} \cdot \Delta\overline{P_1N_1} \quad (3)$$

$$M_{P2} = - C_S \cdot d_{Qx,2} \cdot \Delta\overline{P_2N_2} \quad (4)$$

The preload distances are generated by DC motors ⑧. They allow in-situ adjustment and readjustment during the measurement. A self-locking screw gear secures the set position. Adjustable counterweights ⑨ are attached to the measurement lever to compensate for the geometric stiffness caused by the masses of the links. By adjusting the center of gravity close to the pivot point H, the geometric stiffness is minimized down to almost zero for yaw and roll motions. Minor changes in the geometric stiffness due to a pitch motion must be compensated for by the submechanisms. A second option is to compensate for the entire geometric stiffness along with the elastic stiffness by an in-situ adjustment before every measurement. Both variants enable constant properties regardless of the orientation.

The geometry and material parameters (Table 1) have been iteratively optimized to allow the concept to be implemented in a minimum design space.

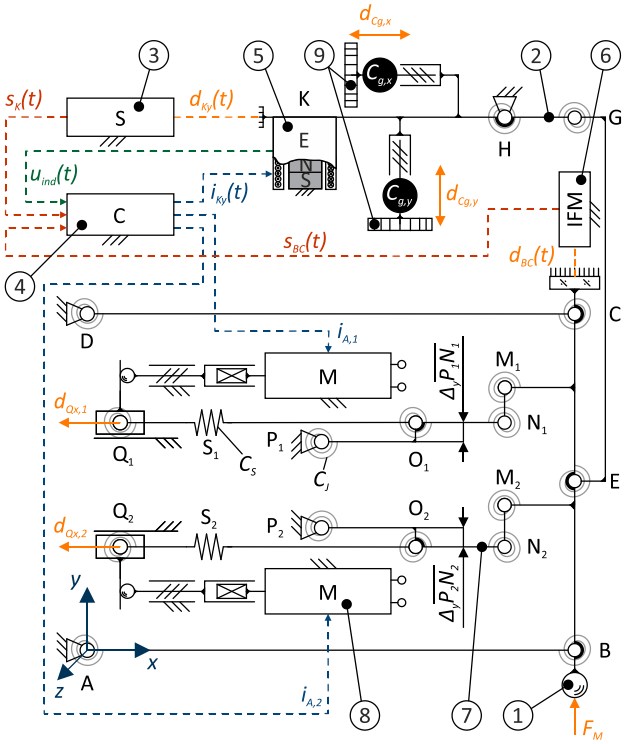

Figure 1. Concept of the developed sensor PROT-MFS.

Table 1. Property-defining geometry parameters and elastic stiffnesses of the deforming elements of the force sensor.

Parameter	Value	Parameter	Value
AB_x, CD_x	90 mm	NS_x	52.8 mm
AD_y, BC_y	70 mm	NQ_x	70.6 mm
EG_y	45 mm	$\Delta_y P_1 N_1$	- 1 mm
HG_x	15 mm	$\Delta_y P_2 N_2$	1 mm
HK_x	55 mm	E	135 GPa
MN_y	40 mm	υ	0.33
NO_x	15 mm	C_J	11.84 Nmm/rad
NP_x	36 mm	C_S	122.67 N/mm

3.2. Design

The force sensor is designed following the principle of function material at the function location (Figure 2). The forces to be measured are applied to a probe ① with a ruby sphere tip of high wear resistance and dimensional stability. The kinematic structure ② is implemented as a non-monolithic compliant mechanism with concentrated leaf spring joints made of copper beryllium. This material has a high strength and nearly linear elastic behavior. The links between the joints are made of aluminum alloy to keep the mass low. To compensate for the

geometric stiffness, adjustable symmetrical brass bodies ⑨ are provided. A position sensor ③ based on a double photodiode, a LED and a slit on the measurement lever detects the deflection during the process. The compensation force is generated by a voice coil actuator ⑤ to implement the desired measurement range of 100 mN. The actuator also includes mechanical stops to avoid plastic deformations. There is also a transportation lock provided ⑫. A fixed fiber interferometric sensor [11] and a mirror mounted to the coupler of the parallel crank ⑥ are used for the actuator calibration in Velocity Mode. A flexure-based mount ⑪ implements the required adjustments for the fiber interferometric sensor.

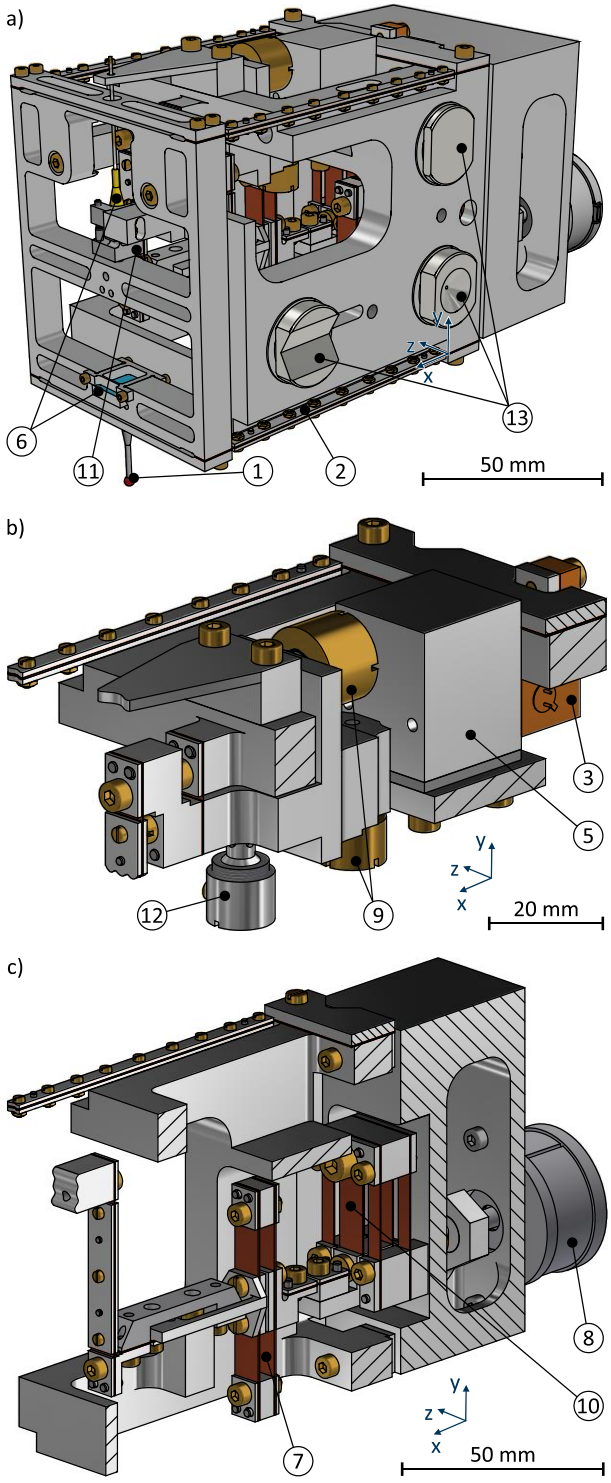

Figure 2. Mechanical design of the developed sensor. a) Side view of the system. b) Section view on the measurement lever assembly c) Section view on the stiffness compensation assembly.

DC flat motors ⑧ combined with fine lead screws generate the preload motions for the compensation springs ⑦. A positioning resolution of better than 1 µm is achieved with minimal design space. Nested double parallel spring guide configurations ⑩ realize the translatory preload motions. Thus, the parasitic lateral motions of single parallel spring guides are reduced to almost zero. A kinematic coupling ⑬ is provided for the statically determined attachment of the force sensor.

4. Simulation results

The compliant kinematic structure was investigated using the Finite Element Method. The relationship between the force F_{Ky} and the displacement d_{Ky} at the operation point K of the ideal system is shown across the entire compensation range (Figure 4) and around zero stiffness (Figure 5).

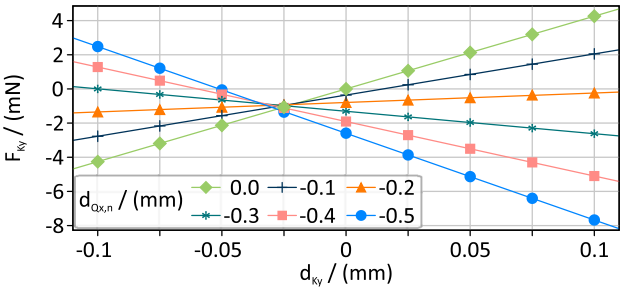

Figure 3. Force displacement diagram at the operation point K across the entire compensation range of up to $d_{Qx,n}$ = -0.5 mm.

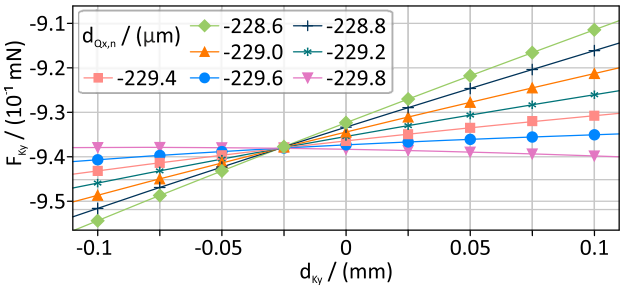

Figure 4. Force displacement diagram at the operation point K in the working range around zero stiffness.

To characterize the function-limiting shift of the measurement window due to manufacturing deviations at the compensation mechanisms [10], a Monto Carlo simulation was carried out (Figure 5). The simulation considered the y-positions of the joints N, O, P, and Q and the spring S. The tolerance range was estimated at ± 100 µm around the ideal position according to ISO 2768-1. The impact was evaluated using the force F_{Ky} required at operation point K to keep the measurement lever in the neutral position d_{Ky} = 0 mm. The preload distances were selected at $d_{Qx,n}$ = -228.6 µm for each simulation run to compensate for the stiffness in the desired range.

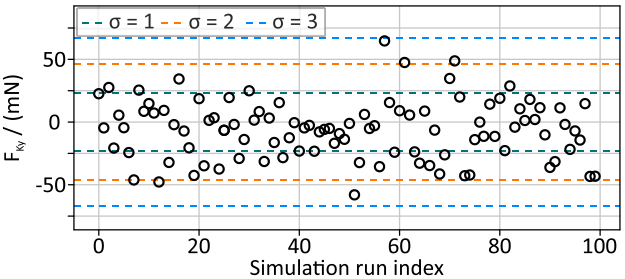

Figure 5. Scattering of the required force F_{Ky} for zero deflection d_{Ky} at the operation point K with an initiated preload distance of $d_{Qx,n}$ = -228.6 µm for varying y-positions of the joints N, O, and Q and the springs S.

The scatterings due to manufacturing deviations of the initial stiffness C, the preload distances $d_{Qx,n}$ for zero stiffness, and the maximum stress σ_{max} (Figure 6) were determined by a Monte Carlo simulation. Therefore, the thicknesses of the joints and the compensation springs varied within the tolerances provided by the manufacturer. The thickness tolerances provided by the manufacturer are for the bending joints from 50 µm to 100 µm, and for the leaf spring elements from 297 µm to 303 µm.

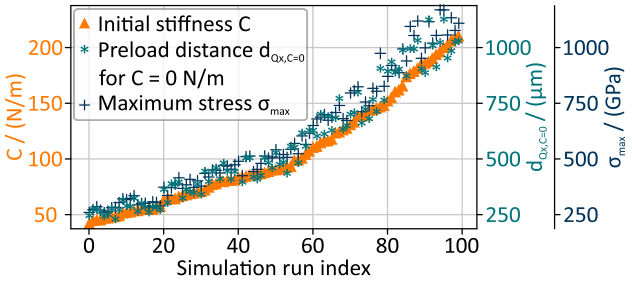

Figure 6. Scattering of the initial stiffness C, the preload distance $d_{Qx,C=0}$ for zero stiffness, and the maximum equivalent stress σ_{max} under variation of the thicknesses of the bending joints and the leaf spring elements of the compensation spring.

5. Discussion

The results of the Finite Element simulations confirm the force sensor concept. Preloading the compensation springs enables an adjustment of the stiffness. Even negative values can be set. The force-displacement diagram across the entire compensation range (Figure 3) shows that there are generally linear correlations between the stiffness of the mechanism and the initiated preload distance as well as for force and deflection. In the working range around zero stiffness, the force-displacement curve has a slightly non-linear trend (Figure 4). For the described design, the highest positive residual stiffness is achieved at a preload distance of $d_{Qx,n}$ = -228.6 µm. The initial stiffness can thus be reduced from 42.58 N/m to at least 0.22 N/m. With the position detection sensitivity of the photodiode sensor of 1 nm at the operation point K and transmission ratio 4, forces F_M of 880 pN can be resolved. A further improvement of the preload resolution enables even higher force resolutions. Differences to the simulation results of the rigid body model [12] were found to result from the complex bending of the joints P_1 and P_2.

In the force-displacement diagrams a negative offset force F_{Ky} can also be seen at zero deflection d_{ky} after initiating identical preload distances $d_{Qx,n}$ at both compensation springs. This offset force can also be explained by the asymmetrical complex bending of the joints P_1 and P_2 under the preload force. It results in an initial deflection and thus a shift of the measurement window. Evenly opposing readjustment of the preload distances reduces this offset force to nearly zero while maintaining the desired stiffness value. The scattering of the offset force was analyzed considering the critical manufacturing deviations at the compensation mechanism (Figure 5). For $\sigma = 1$, the range is ±23.28 mN and for $\sigma = 2$, it is ±46.58 mN. On average, the offset is slightly negative at -6.18 mN. For small deviations of the positions (Figure 5 green and orange separation lines), a distribution around the mean value can be observed. Larger deviations (Figure 5 blue separation line), scatter relatively evenly around 0 mN. Examining the impact of thickness deviations from manufactured revolute joints and the compensation spring elements (Figure 6) reveals, that the stiffness adjustment concept generally works in the entire tolerance range. However, a large thickness of the bending joints leads to a high initial stiffness. To compensate for this, enlarged preload distances are required, which cause higher internal stresses. Special high strength alloys are necessary. Systems with joint thicknesses between 80 µm to 100 µm exceed the stress of 800-900 GPa and thus are likely to fail during operation. Manufacturing deviations of the joint positions in the compensation mechanism lead to an uneven spring preload to enter the measuring window. The material stress in one of the critical leaf spring elements is thus increased. As a consequence, variations in the leaf spring thicknesses have to be further reduced.

6. Summary and Outlook

The redefinition of the SI unit Kilogram allows for directly traceable force and mass measurements while reducing measurement uncertainty. This paper presents the concept and design of a force sensor for high-precision force metrology and micro- and nanofabrication applications. It is based on the Planck Balance. Two spring-based mechanisms are used to compensate for the elastic stiffness of the compliant kinematic structure and minor geometric stiffnesses caused by the link masses. Numerical investigations show that the concept allows a perfect stiffness reduction, practically down to at least 0.5% of the initial value. The impact of manufacturing deviations is also eliminated by the stiffness adjustment. The achievable force resolution for the given design is below 880 pN but can be further increased by design measures. Investigations of the effects of manufacturing deviations show that the initial stiffness in particular must be kept low to avoid high stresses in the system.

In further work, the force sensor will be manufactured, put into operation, and investigated experimentally. After the successful validation of the concept, the sensor will be integrated into a target application.

Acknowledgment

The authors gratefully acknowledge the support of the Deutsche Forschungsgemeinschaft (DFG) within the framework of the Research Training Group “Tip- and laser-based 3D-Nanofabrication in extended macroscopic working areas” (GRK 2182) at the Technische Universität Ilmenau, Germany.

References

[1] Robinson I A, Schlamminger S 2016 *Metrologia* **53** 5 A46–A74

[2] Rothleitner C, Schleichert J, Rogge N, Günther L, Vasilyan S, Hilbrunner F, Knopf D, Fröhlich T, Härtig F 2018 *Measurement Science Technology* **29** 7 074003

[3] Li Z, Zhang Z,Lu Y, Hu P, Liu Y, Xu J, Bai Y, Zeng T, Wang G, You Q, Wang D, Li S, He Q, Tan J 2017 *Metrologia* **54** 5 763-774

[4] Dannberg O, Kühnel M, Fröhlich, T 2020 *Technisches Messen* **87** 10 622-629

[5] Mayworm R C, Webster E, Davidson S, Alvarenga A V, Costa-Felix R P B 2022 *Measurement* **203** 111788

[6] Günther L., Rothleitner C, Schleichert J, Rogge N, Vasilyan S, Härtig F, Fröhlich T 2018 *Journal of physics* **1065**

[7] Bacher J P, Joseph C, Clavel R 2002 *Ind. Robot* **29** 349–353

[8] Hilbrunner F, Rahneberg I, Fröhlich T 2018 T*echnisches Messen* **85** 11 658-679

[9] Torres Melgarejo M A, Wittke M, Theska R 2022 *Proceedings of the 22nd International Conference of the European Society for Precision Engineering and Nanotechnology* 67-68

[10] Wittke M, Torres Melgarejo M A, Darnieder M, Theska R 2023 *Engineering for a changing world: Proceedings: 60th ISC, Ilmenau Scientific Colloquium, Technische Universität Ilmenau, Germany*

[11] Shmagun V, Vasilyan S, Rogge N, Fröhlich T, Kissinger T 2023 *Measurement Science Technology* **34** 12 125017

[12] Wittke M, Torres Melgarejo M A, Wolf M, Fröhlich T, Theska R 2025 *Proceedings of the Sensor and Measurement Science International Conference (SMSI)* A4.2